OAK RIDGE
NATIONAL LABORATORY
MANAGED BY UT-BATTELLE
FOR THE DEPARTMENT OF ENERGY

NFE-09-02126

Division

CRADA Final Report
For
CRADA Number NFE-09-02126

Multiscale Toxicology- Building the Next Generation Tools for Toxicology

Scott T. Retterer
Oak Ridge National Laboratory

Michael P. Holsapple
Battelle Memorial Institute

Prepared by
Oak Ridge National Laboratory
Oak Ridge, TN 37831
managed by
UT-BATTELLE, LLC
for the
U.S. Department of Energy
under contract DE-AC05-00OR22725

Approved for Public Release

UT-BATTELLE
ORNL-27 (4-00)

Abstract

A Cooperative Research and Development Agreement (CRADA) was established between Battelle Memorial Institute (BMI), Pacific Northwest National Laboratory (PNNL), Oak Ridge National Laboratory (ORNL), Brookhaven National Laboratory (BNL), Lawrence Livermore National Laboratory (LLNL) with the goal of combining the analytical and synthetic strengths of the National Laboratories with BMI's expertise in basic and translational medical research to develop a collaborative pipeline and suite of high throughput and imaging technologies that could be used to provide a more comprehensive understanding of material and drug toxicology in humans. The Multi-Scale Toxicity Initiative (MSTI), consisting of the team members above, was established to coordinate cellular scale, high-throughput *in vitro* testing, computational modeling and whole animal *in vivo* toxicology studies between MSTI team members. Development of a common, well-characterized set of materials for testing was identified as a crucial need for the initiative. Two research tracks were established by BMI during the course of the CRADA. The first research track focused on the development of tools and techniques for understanding the toxicity of nanomaterials, specifically inorganic nanoparticles (NPs). ORNL's work focused primarily on the synthesis, functionalization and characterization of a common set of NPs for dissemination to the participating laboratories. These particles were synthesized to retain the same surface characteristics and size, but to allow visualization using the variety of imaging technologies present across the team. Characterization included the quantitative analysis of physical and chemical properties of the materials as well as the preliminary assessment of NP toxicity using commercially available toxicity screens and emerging optical imaging strategies. Additional efforts examined the development of high-throughput microfluidic and imaging assays for measuring NP uptake, localization, and toxicity *in vitro*. The second research track within the MSTI CRADA focused on the development of *ex vivo* animal models for examining drug-induced cardiotoxicity. ORNL's role in the second track was limited initially, but was later expanded to include the development of microfluidic platforms that might facilitate the translation of Cardiac 'Microwire' technologies developed at the University of Toronto into a functional platform for drug screening and predictive assessment of cardiotoxicity via high-throughput measurements of contractility. This work was coordinated by BMI with the Centre for the Commercialization of Regenerative Medicine (CCRM) and the University of Toronto (U Toronto). This partnership was expanded and culminated in the submission of proposal to Work for Others (WFO) agencies to explore the development of a broader set of microphysiological systems, a so call human-on-a-chip, that could be used for toxicity screening and the evaluation of bio-threat countermeasures.

Statement of Objectives

The objectives of this CRADA are to;

1) Establish a suite of quantitative analysis capabilities that can be used to link toxicity studies across the molecular, cellular and whole animal scales.
2) Position Battelle Memorial Institute and participating DOE laboratories in a leadership position in the fields of Nano- and Predictive Toxicology through the development of

emerging high-throughput and high content in vitro methods for predicting toxicity in the pre-trial phase of chemical and material testing.

3) (ORNL Specific) – establish a library of well-characterized nanomaterials that can be used across the MSTI team to allow correlation of toxicity tests conducted using multiple modes of imaging.

Benefits to the Funding of DOE Office's Mission

The functional nanomaterials and high-throughput screening technologies developed by ORNL during the course of this CRADA are broadly applicable to the DOE Office's Missions associated with efficient energy use and improved health and environmental quality. The methods developed for characterizing the biological systems and materials utilized in this effort provide new insights into the interactions between hard and soft matter. The nanomaterial synthesis techniques developed in this CRADA culminated in the creation of a broad class of core-shell nanoparticles that allow functional NP cores, comprised of noble metals, plasmonic materials, and ferromagnetic metals, to be encapsulated within volume-labeled silica shells that have optically and/or radioactive signatures that facilitate tracking in cellular and whole animal models. Surface modifications to the particles allow targeting of NPs to specific biological targets and are crucial to conducting rigorous fundamental studies to determine how these particles interact with soft materials.

The broad benefits of the CRADA work to the improvement of health and environmental quality are inherent in the overall objective of the work to develop more comprehensive understanding of nanomaterial toxicity. A more detailed understanding of the health and environmental impact will poise DOE and affiliated laboratories to address environmental safety and health questions related to the large scale manufacturing and dissemination of nanomaterials in commercial products ranging from drug delivery vehicles, and solar panel components to active optically active compounds in cosmetic products. High-throughput screening technologies based on microscale tissue models may contribute to the development of low-cost, low-risk platforms for monitoring environmental safety.

Technical Discussion

The CRADA objective "to develop a toxicity testing pipeline using quantitative techniques and next generation tools that combine insights into the molecular mechanisms responsible for the toxicity of nanomaterials and identification of target cells and organs," is underpinned by a need to perform such studies and qualify the tools of interest using carefully synthesized and characterized nanomaterials. There is a great deal of seemingly inconsistent, if not overtly contradictory, material within the literature describing the 'toxicity' of specific classes of nanomaterials. Such contradictions can, to a large extent, be attributed to slight differences in NP synthesis and purification. Also, discrepencies in the concentration (mass/Volume) and size distribution of commercial products can vary significantly from one batch to the next. In order to address the goals of the project, monitoring the fate and impact of nanomaterials across the molecular, cellular, and whole animal scale using multiple imaging and characterization technologies including Magnetic Particle Dosimetry (MPD) (PNNL), ultra-high resolution fluorescence microscopy (PNNL & ORNL), Accelerator Mass Spectroscopy (AMS) (LLNL), and

Positron Emission Tomography (PET) (BNL), NPs with radio, optical and ferromagnetic signatures needed to be developed. To allow the correlation of results across the imaging modalities chosen, the size, shape and surface functionality of the particles needed to remain constant. Also, because many of the participating labs were not prepared to work with radioactive particles (C14-labeled), 'hot' and 'cold' (non-radioactive) particles were produced. Results across the project were based on the hypothesis that particles of the same size, shell, and surface composition would behave identically *in vitro* and *in vivo*. ORNL developed a unique solution to address this challenge, developing a core-shell synthesis process that allowed the creation of silica and silica shell NPs in which the radio- and optical labels could be covalently incorporated into the silica structure. The particles exhibited exquisite stability and were amenable to surface modification. Manuscripts describing the synthesis and characterization of these particles are currently in preparation or in review. Summaries of the manuscripts and some of the primary figures (adapted from these manuscripts) are provided below.

Adapted from **Volume Labeling with Alexa-Fluor Dyes and Surface Functionalization of Highly Sensitive Fluorescent SiO_2 Nanoparticles** accepted in Nanoscale, June 2013

A new synthesis approach is described that allows the direct incorporation of fluorescent labels into the volume or body of SiO_2 nanoparticle. In this process, fluorescent Alexa Fluor dyes with different emission wavelengths were covalently incorporated into the SiO_2 nanoparticles during their formation by the hydrolysis of tetraethoxysilane. The dye molecules were homogeneously distributed throughout the SiO_2 nanoparticles. The quantum yields of the Alexa Fluor dyes within the volume-labeled SiO_2 nanoparticles were much higher than nanoparticles labeled using conventional organic dyes. The size of the resulting nanoparticles was controlled using microemulsion reaction media with sizes in the range of 20-100 nm and a polydispersity that was less than15%. In comparison with conventional surface tagged particles created by post-synthesis modification, this process maintains the physical and surface chemical properties that have the most pronounced affect on colloidal stability and interactions with their surroundings. These volume-labeled nanoparticles, as a result of the covalent integration of functional molecules into particle body, have proven to be extremely robust, showing excellent signal strength, negligible photobleaching and minimal loss of functional organic components. The native or "free" surface of the volume-labeled particles can be altered to achieve a specific surface functionality without altering fluorescence. Their utility was demonstrated for visualizing the association of surface modified fluorescent particles with cultured macrophages. Differences in particle agglomeration and cell association were clearly associated with differences in observed nanoparticle toxicity. The capacity to maintain particle fluorescence while making significant changes to surface chemistry makes these particles extremely versatile and useful for understanding the effects of surface charge on particle agglomeration, uptake, and transport in environmental or biological systems.

Recently, a series of relatively new fluorescent molecules have been developed by sulfonating aminocoumarin, rhodamine, or carbocyanine dyes, referred as Alex Fluor dyes. The excitation and emission wavelength ranges of Alexa Fluor dyes cover the entire spectrum from ultraviolet to red. These dyes exhibit higher brightness, more photostability and less quenching upon bioconjugation than cyanine stains, as well as pH insensitivity over a very broad range. The

performance of Alexa dyes has also been demonstrated to be superior to that of the commonly used dyes in various bioapplications, especially at high degrees of labeling. In this research, we developed a new approach to homogeneously graft the Alexa Fluor molecules into SiO_2 nanoparticles through covalent bonding. The synthesized fluorescent SiO_2 particles exhibit a number of significant advantages as fluorescence probes: (i) increased fluorescence intensity, (ii) enhanced photostability, (iii) highly uniform and tunable particle size, and (iv) availability of the native "free" surface for further modification.

In a typical synthesis reaction using amine reactive dyes, 2.5 mg succinimidyl ester of Alexa Fluor dye is combined with 0.25 g APTES in 10 mL cyclohexane and reacted under stirring for 3 hours; then the dye-APTES was mixed with 9.3 mL of TEOS and added into the microemulsion reaction media, following the reaction as described in the experimental section of the manuscript. The as-synthesized fluorescent SiO_2 nanoparticles were obtained with sizes of 32 nm and 76 nm by using the microemulsion I and II systems respectively. Similar procedures were used for incorporating thiol reactive dyes, in which 2.5 mg maleimide and 0.25 g MPTMS were first reacted in 1 mL DMSO. The resulting fluorescent SiO_2 nanoparticles have a broader size distribution than those synthesized using amine reactive dyes, having a polydispersity greater than15%. Thus, the following discussion focuses on nanoparticles synthesized with amine reactive dyes. Figure 1 shows SEM images of the synthesized SiO_2 nanoparticles with Alexa Fluor 430 succinimidyl ester. The particles show uniform size with a polydispersity < 10%.

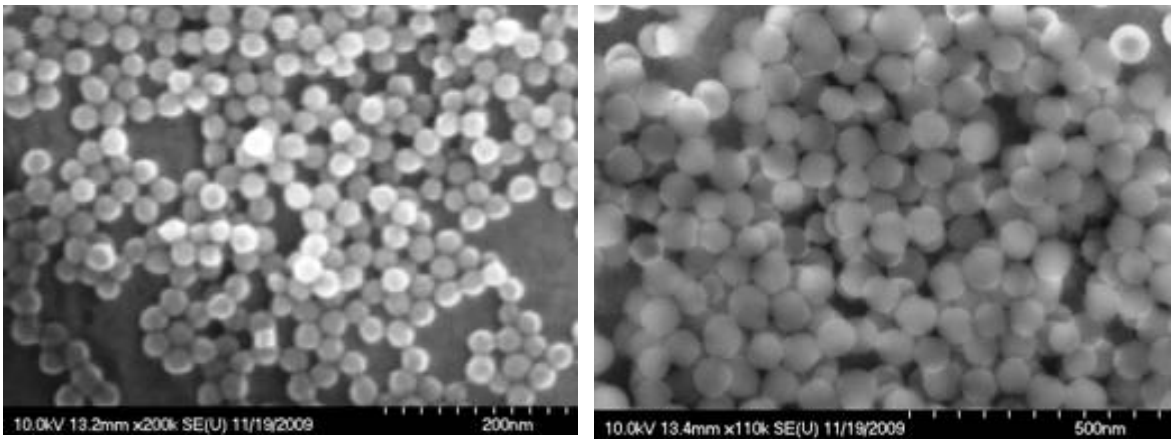

Figure 1. SEM images of Alexa Fluor 430 labeled SiO_2 nanoparticles, (left) <d>=32 nm, σ=±2.9 and (right) <d>= 76 nm, σ=±4.8.

As shown by UV-Visible spectra in Figure 2, the absorption properties remain unchanged between free dye molecules and those within the SiO_2 nanoparticles, implying the dye molecules are stable throughout the chemical synthesis process.

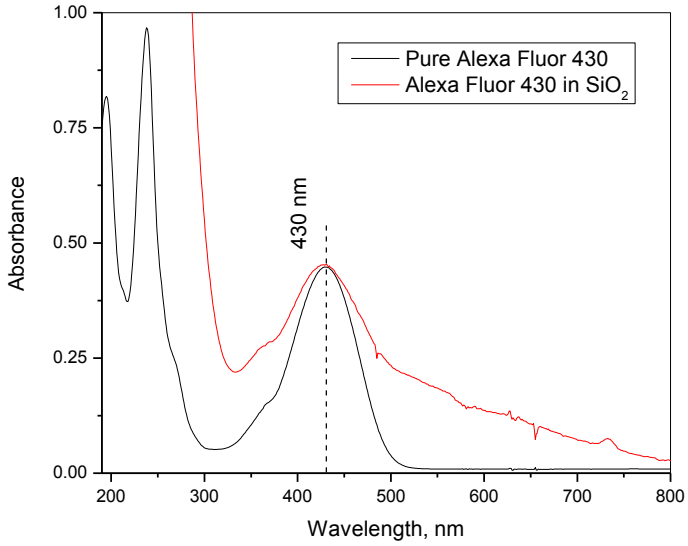

Figure 2. Absorption spectra of (a) pure Alexa Fluor 430 succicimidyl ester in water and (b) Alexa Fluor 430 labeled SiO_2 nanoparticles (32-nm) in DMSO. The DMSO was used as solvent to match refractive index of SiO_2 for eliminate light scattering from the colloidal suspension for the absorption spectral measurement.

The fluorescence intensities of the Alexa Fluor dye labeled SiO_2 nanoparticles in suspension were measured at different nanoparticles concentrations. As shown in Figure 3, fluorescence can be readily detected even at nanoparticle concentrations below ng/mL levels, demonstrating high sensitivity of the volume-labeled nanoparticles.

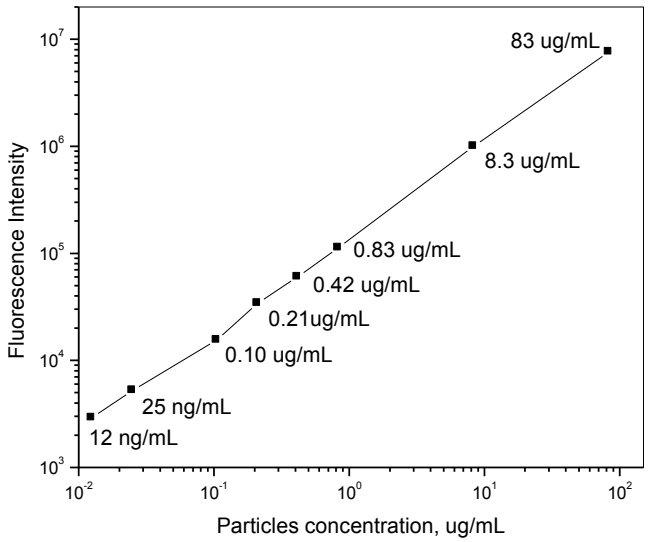

Figure 3. Fluorescence intensities at 535-nm of Alexa Fluor 430 labeled 32-nm SiO_2 nanoparticles at different concentrations in water

(excitation at 430-nm). Fluorescence is stable and readily detectable at ng/mL levels.

During synthesis, ~0.1wt% of dye molecules were introduced into the SiO_2 nanoparticles. Because the Alexa Fluor dyes are charged molecules, the effects of the doped dyes on colloidal dispersion and charge density were evaluated through dynamic light scattering and zeta potential (ζ) measurements at pH ~7 (Table 1).

Table 1. Hydrodynamic sizes and zeta potentials and plain and Alexa Fluor dye doped SiO_2 nanoparticles before and after surface functionalization

SiO_2 Nanoparticles*	Size (nm) ± polydispersity (%)			ζ (mV) ± half width (mV)		
	Non-modified	-COOH modified	$-NH_2$ modified	Non-modified	-COOH modified	$-NH_2$ modified
Plain	37.4±7.2	38.2±8.8	361±27.1	-38.3±3.6	-49.5±4.2	16.5±4.5
AF 350 labeled	62.4±11.2	38.9±9.7	574±23.6	-32.1±3.3	-48.2±3.7	20.1±4.1
AF 430 labeled	78.8±14.2	39.6±9.2	688±24.2	-30.7±3.4	-43.8±4.6	11.8±4.3
AF 488 labeled	68.2±13.8	38.5±7.9	721±26.6	-36.8±3.2	-44.3±3.3	12.2 ±4.2
AF 532 labeled	72.1±14.7	40.6±9.8	701±22.5	-41.2±3.7	-47.6±4.1	18.2±3.7

*Average particle sizes are 32±2.5nm determined by SEM images. The DLS and ζ measurements were performed in 1mM KCl solution at pH=7.0±0.2.

The volume labeled SiO_2 nanoparticles are very stable in suspension as a result of the covalent bonding of the Alexa Fluor dyes to SiO_2. The Alexa Fluor dye molecules exhibit very little leaking and negligible photobleaching in the SiO_2. An example fluorescence image from 78-nm Alexa Fluor 488 dye labeled SiO_2 nanoparticles is shown in Figure 4. The image was taken after the synthesized nanoparticles have stood in dark for 18 months.

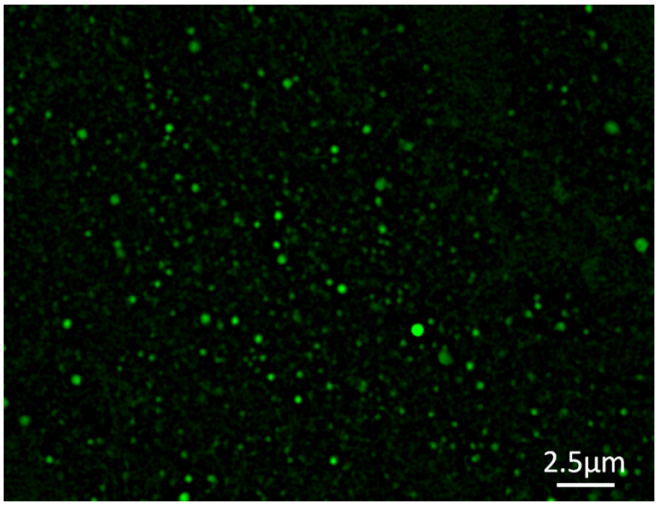

Figure 4. Fluorescence image of Alexa Fluor 488 labeled 76-nm SiO_2 nanoparticles. The nanoparticle suspension has been stood in dark for 18 months before the measurement.

For the volume labeled SiO_2 nanoparticles, one of the major advantages is that surfaces of SiO_2 remain free for additional surface modification. Directed modification of nanoparticle surfaces is crucial for controlling interactions of particles with each other and their surrounding environment.

This is of particular importance in interpreting the fate and impact of particles interacting with biological and environmental systems.

As indicated by ζ potentials in Table 1, with all studied Alexa Fluor dyes, the surface modification with $–COO^-$ groups enhanced negative charge density of the resulting SiO_2 colloidal nanoparticles while surface modification with $–NH_2$ groups converted the surface charge to positive at near neutral pH. High negative surface charges made the colloidal suspension highly stable because of strong repulsive force between particles. Since $–NH_2$ modification lowered surface charge density and the $–(CH_2)_3\text{-}NH_2$ groups make the surface more hydrophobic, the $–NH_2$ modified nanoparticles showed increased aggregation corresponding with increased hydrodynamic particle size measurements. While a full analysis of the effects of surface charge on nanoparticle toxicity is beyond the scope of this manuscript, Figure 5, illustrates the utility of the volume labeled and surface modified particles in modulating and tracking nanoparticle-cell interactions. The $–NH_2$ surface modifications clearly lead to particle aggregation and settling that significantly increases nanoparticle toxicity compared with the well dispersed COO- modified particles.

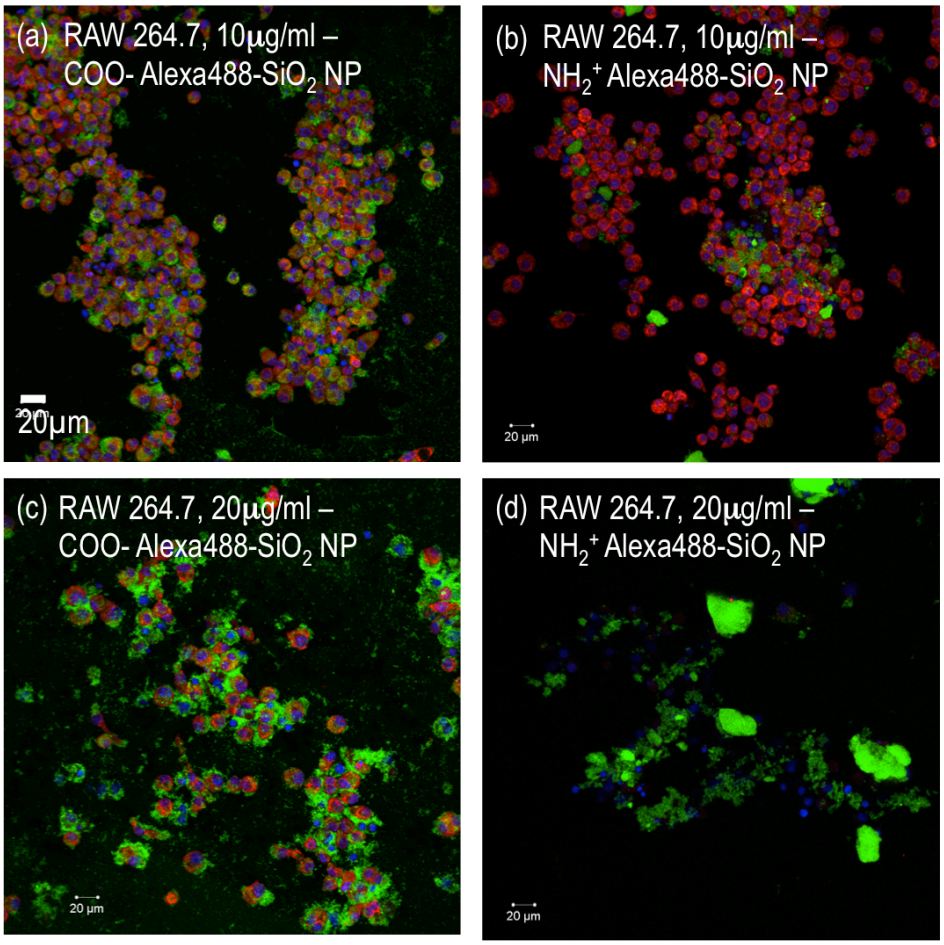

Figure 5. Alexa Fluor 488-SiO_2 nanoparticles associated with murine macrophage cells in culture. Aggregation of $–NH_2$ functional nanoparticles (b,d) likely contributes to settling and cell death. Large aggregates of fluorescent particles are observed compared to well dispersed $–COO^-$ functional particles.

Adapted from **Unique Surface Radiolabeling Scheme of Super Paramagnetic Iron Oxide Nanoparticles (SPIONs) for Accurate Extrapolation of Pharmaco-Kinetic Distribution Studies in Life Sciences,** manuscript in preparation for submission to Nanoscale.

Biological efficacy of any nanobased system is dependent on bio-distribution and bio absorption. In this study we used a unique radiolabeling approach to incorporate ^{14}C on to the surface of an iron based hydrophilic nanoparticle system. The *in vivo* bio-distribution was determined by detecting ^{14}C labels ($t_{1/2}$=5730 years) that were incorporated into the organic functional groups on the surface of the nanoparticles using Accelerator Mass Spectroscopy (AMS). This approach provides comparable data sets on account of the radio-labeled probes having the same chemical properties as the non-labeled probes that they were intended to mimic. This is a very significant aspect of the radio labeling approach used in these studies. Since, the synthesis approach described here is broadly applicable to the synthesis of nanoscale materials with multiple core and surface functionalities, this work combined with the pharmacokinetic data suggests that these nanoparticles have broad implications for use in biological applications as therapeutic, diagnostic or even theragnostic agents.

For bio-distribution studies, the preferred mode of delivering the molecule of interest, *in vivo* is either intra-venously or through inhalation.[11] (Rabanel, J. M.; Aoun, V.; Elkin, I.; Mokhtar, M.; Hildgen, P., Drug-loaded nanocarriers: passive targeting and crossing of biological barriers. *Curr Med Chem* **2012,** *19* (19), 3070-102.)To allow for dual delivery modes of NPs in vivo, the hydrodynamic radius of the magnetic nanoparticles in this study was optimized to be between 75-100 nm by attempting different functionalization schemes. The most stable nano-carrier system we designed were water dispersed iron oxide nanoparticles (~10 nm) with branched carboxylic acid (-COOH) functional groups. Once we optimized size and chemical stability of nanoparticles in solution, the *in vitro* nanotoxicity of non-radio labeled nanoparticles was determined using RAW 264.7 macrophage cells and C10 mouse lung epithelial cells. To ensure that the NPs used in the *in vivo* pharmacokinetics study have the same physical and chemical properties as the NPs used in the *in vitro* toxicity study, a unique approach to radiolabeling the nanoparticles was utilized here by incorporating ^{14}C, a beta emitter ($t_{1/2}$=5730 years), into the organic functional groups, with the radioactivity controlled at ~ 0.1 nCi/mg. This novel radiolabeling scheme enabled us to determine in vivo distribution in a mouse model system using Accelerator Mass Spectroscopy (AMS) with precise pharmacokinetic metrics. This radio-labeling approach studies was significant, as the NPs probes had the same chemical properties as the non-labeled probes that they were intended to mimic. The nanoparticles synthesized in this work have implications for use in different biological applications and the approach described is broadly

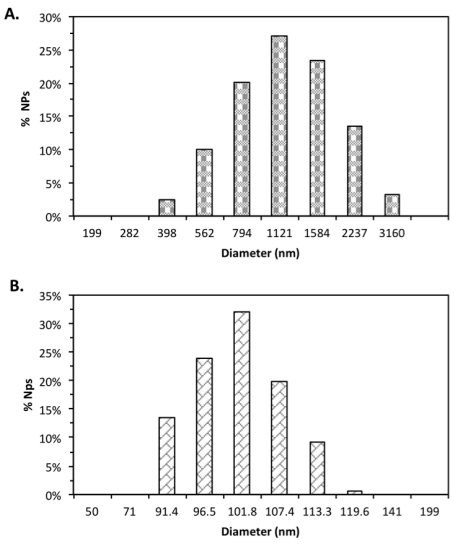

Figure 6: The cluster size of NPs in solution was determined using DLS. **(A)** The cluster size of FeII/FeIII NPs in water was 1110.9 ± 483.3 nm and **(B)** the cluster size of FeII/FeIII NPs after functionalization with N-[(3-trimethoxysilyl)propyl]ethylenediamine triacetic acid tripotassium salt was 101.73 ± 19.4 nm

applicable to the synthesis of nanoscale materials with multiple core and surface functionalities.

Iron oxide NPs are superparamagnetic and tend to agglomerate in solution to form viscous magnetic fluids. DLS measurements of FeII/FeIII NPs in water indicate agglomerate sizes of 1110.9 ± 483.3 which is in the millimeter regime (Fig.7A). The size of these agglomerates limits their suitability for biomedical applications. After silanizing the surface of the nanoparticles with Si-EDTA, DLS measurements indicated agglomerate sizes of 101.73 ± 19.4 nm (Fig.7B).

In order to track the in vivo bio-distribution of the nanoparticles with high sensitivity, it is necessary to tag the NPs with a suitable radiolabel that can be detected by an ultra-sensitive analytical tool like Accelerator Mass Spectrometer. ^{14}C labels were incorporated into the carboxylate functional group (–COOH) in Si-EDTA which are covalently linked to the surface of NPs. ^{14}C is a beta emitter with a ($t_{1/2}$=5730 years) that can be easily detected at ultra-low concentrations (10^{-18}) using mass spectroscopy. The reaction employed was adapted from the commercial synthesis of EDTA from Ethylenediamine. However, this application is the first time that the reaction has been optimized to occur on the surface of FeII/FeIII nanoparticles. We achieved radioactivity of 0.097 nCi/mg of NPs sample, which was used for the *in vivo* bio-distribution studies. The radioactivity was tunable up to 100 nCi/mg by using a ^{14}C source with higher specific radioactivity (5 mCi). The reaction method demonstrated here was broadly applicable as the same ^{14}C source can be used in slightly modified reaction schemes to tweak the surface functionalization of the NPs like –COOH functional groups with different lengths of organic chains.

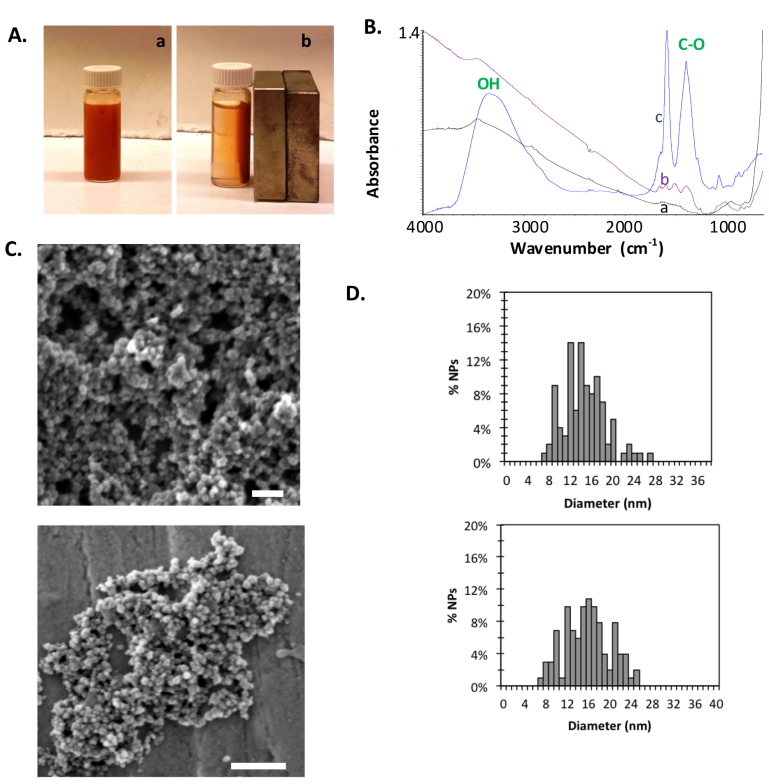

Figure 7: Chemical and Physical characterization of iron-oxide nanoparticles. **(A)** Fe3O4-EDTA nanoparticles (a) dispersed in water and (b) sticking to the side of the glass vial when a magnet is introduced.**(B)** Ft-IR spectra of (a) Fe-Si-diamine NPs alone (medium strength signals for C-N: 1000-1250 cm^{-1} and NH_2 scissoring : 1550-1650 cm^{-1}; Weak signals from NH_2 of 1^0 amines and NH of 2^0 amines : 3300-3500 cm^{-1}) (b) Fe-Si-diamine NPs with some acetic acid groups substituted into the amines and (c) Fe-Si-diamine NPs with completely converted ethylene diamine to ethylenediamine triacetic acid. Medium to strong signals from –C-O are at 1210-1320 cm^{-1} and –OH lines are broad and at 2500-3300 cm^{-1}. **(C)** SEM images of (a) FeII/FeIII NPs alone and (b) Fe-Si-EDTA NPs. **(D)** The core size distribution of (a) FeII/FeIII NPs was 14.08 ± 3.92 nm and (b) Fe-Si-EDTA NPs were 15.31 ± 4.2 nm. All scale bars are 100 nm.

Non-radiolabeled nanoparticles were prepared using the same reaction schemes by using KCN as

the nitrile source for –COOH synthesis (Fig. 7C). The nanoparticles were well dispersed in solution and super paramagnetic (Fig.8A). FT-IR spectra of Fe-Si-Diamine, Fe-Si-diamine partially converted to Fe-Si-EDTA and Fe-Si-diamine completely converted to Fe-Si-EDTA shows the evolution of formation of –COOH groups which replace the hydrogen in the amine groups (Fig.7B). Fe-Si-diamine NPs alone exhibit medium strength signals for C-N between 1000-1250 cm^{-1} and NH_2 scissoring between 1550-1650 cm^{-1}. Weak signals from NH_2 of 1^0 amines and NH of 2^0 amines are located between 3300-3500 cm^{-1} . Fe-Si-diamine NPs after partial substitution of amine groups with acetic acid groups show the appearance of distinct peaks associated with –C-O between 1210-1320 cm^{-1}. After complete conversion of ethylene diamine on Fe-Si-Diamine NPs to ethylenediamine triacetate, medium to strong signals from –C-O are recorded between 1210-1320 cm^{-1} and –OH lines at 2500-3300 cm^{-1} are broad. Zeta potential of Fe-Si-EDTA was measured at -37.73 ± 2.39 mV. This is indicative of highly stable NPs. SEM measurements showed core size distributions of 14.08 ± 3.92 nm for Fe_3O_4 NPs and 15.31 ± 4.32 nm for Fe-Si-EDTA NPs (Fig.7 C-D).

The chemical toxicity of non-labeled Fe-Si-EDTA NPs was tested against two cell lines. The cell lines used were C10 murine lung epithelial cells and RAW 264.7 macrophage cells. The viability of the cell lines was assessed using LDH and MTT 24 hours after exposure to nanoparticles. Five concentrations were utilized ranging from 0-200 μg/ml of NPs. These concentrations were chosen in order to cover all possible dosage ranges for both inhalation and intravenous modes of delivery. The experimental runs were done in triplicate. Cells incubated in the absence of NPs were the control population. Statistically, the viability of cells dosed with NPs was not different from the control cells population. This clearly indicated that the NPs were not compromising the membrane integrity of the cells and thereby were not affecting cell structure integrity. The mitochondrial activity and thereby the ability of the cell to respire was tested for C10 lung epithelial cells populations (Fig. 8A-b) and RAW 264.7 macrophage cells (Fig. 8B-b) 24 hours post-incubation with NPs using MTT assay. MTT assays were conducted at the same doses. The runs were done in triplicate. Cells incubated with 0 μg /ml of NPs were the control population. Statistically the viability of cells dosed with NPs were not different from the control cell population which were grown in cell culture medium. This clearly indicated that the NPs were not compromising the ability of the cells to respire, which indicated normal cell function was going on as usual. The *in vitro toxicity* assays indicated that the NPs were non-toxic to the test cell population for the concentration ranges tested.

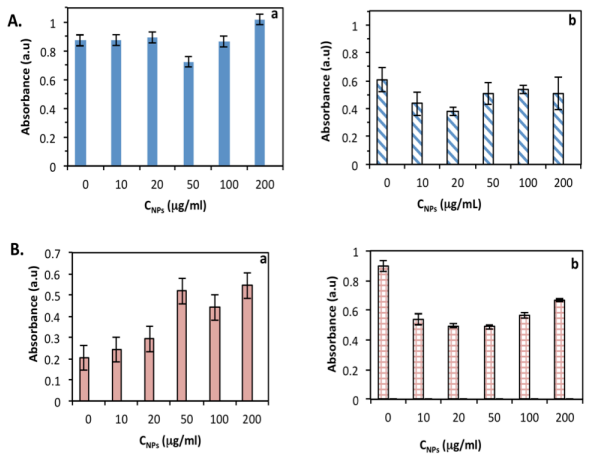

Figure 8: In vitro toxicity assays were done to assess the effect of NPs on cell culture viability. **(A)** C10 lung epithelial cells were tested for cell viability after 24 hours of incubation with NPs using (a) LDH assay and (b) MTT assay. **(B)** RAW 264.7 macrophage cells were tested for cell viability 24 hours post incubation with NPs using (a) LDH assay and (b) MTT assay. The cell population incubated with highest concentration of NPs didn't show any increased toxicity as when compared to the control cell population.

The Stability of radiolabels on Fe_3O_4-Si-($^{14}COO^-$) in saline and fetal bovine serum at room temperature was monitored for a time period of 48 hours (Fig.8A). There was no detectable radioactivity in the supernatant nor was there any significant loss in radioactivity in the nanoparticle fraction. This indicated that the radiolabels were linked stably to the nanoparticles surface in physiological solutions.

0.15 mg of ^{14}C Fe-Si-EDTA NPs nanoparticles were administered intra-venously through the tail over 4 hours at the rate of 37.5 µg /h. The in vivo bio-distribution was determined 30 minutes after the final dose was delivered. Accelerator Mass Spectrometer was used to analyze the Bio-distribution of ^{14}C Fe-Si-EDTA NPs in Mice. The nanoparticles were found distributed throughout the mice with a higher concentration in lungs. This non-specific distribution indicated that the ^{14}C Fe-Si-EDTA NPs and thereby ^{14}C Fe-Si-EDTA NPs will be good drug carrier candidates. The biodistribution after intravenous delivery of NPs at 30 minutes is shown in Figure 9. NPs were found in the phagocytic organs: lung (~400µg/mg), liver (~150µg/mg) and spleen (~200µg/mg). NPs were also observed in the plasma (~50µg/ml).

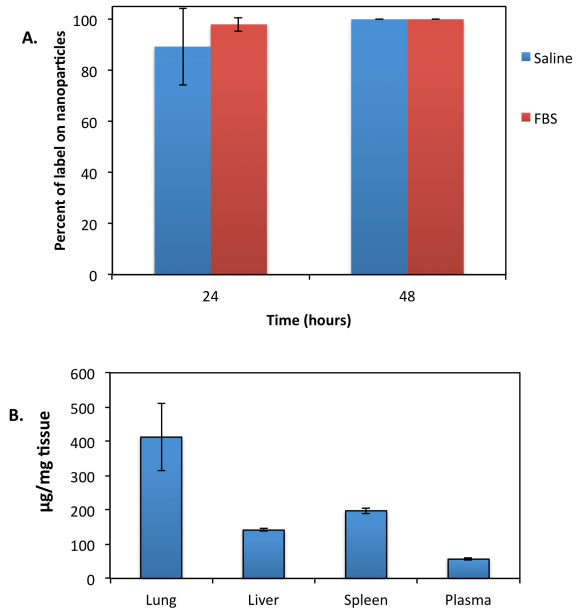

Figure 9: The distribution of ^{14}C labeled NPs in different organs of interest, 30 minutes post intra venous dosage delivery, was detected using AMS. **(A)** The Stability of radiolabels on ^{14}C Fe-Si-EDTA NPs in saline and fetal bovine serum was determined to be stable for at least 48 hours. **(B)** 0.15 mg of tThe ^{14}C Fe-Si-EDTA NPs nanoparticles were administered intra-venously through the tail over 4 hours at the rate of 37.5 mg/h. The in vivo bio-distribution was determined 30 minutes after the final dose was delivered. Accelerator Mass Spectrometer was used to analyze the bio-distribution of ^{14}C Fe-Si-EDTA NPs in Mice. The nanoparticles were found distributed throughout the mice with a higher concentration in lungs. This non-specific distribution indicated that the ^{14}C Fe-Si-EDTA NPs and thereby ^{14}C Fe-Si-EDTA NPs will be good drug carrier candidates.

The nanocluster size of the magnetic nanoparticles was controlled to be between 75-100 nm. The radiolabeling approach used in these studies was significant, as the probes had the same chemical properties as the non-labeled probes that they were intended to mimic. This approach provides useful comparable data sets. The pharmacokinetic data sets were highly accurate as the ^{14}C labeled nanoparticles in tissue samples were detected using Accelerator Mass Spectroscopy (AMS), an ultrasensitive (10^{-18} moles) quantitative spectrometric technique with small sample requirements. This allowed for low dose radio-tagging of nanocarriers with a long lived radiolabel like ^{14}C. The low levels of radioactivity permit long term pharmacokinetic studies without any systemic toxicity from the radiolabel itself. Furthermore, the use of a magnetic core as the nano-carrier for the radiolabels will allow for dual detection schemes, which introduces redundancy into the bio-distribution data.

Adapted from **Dynamic Development of the Protein Corona on Silica Nanoparticles: Composition and Role in Toxicity published Nanoscale** accepted for publication in Nanoscale, May 2013.

The formation and composition of the protein corona on silica (SiO_2) nanoparticles (NP) with different surface chemistries was evaluated over time. Native SiO_2, amine ($-NH_2$) and carboxy ($-COO^-$) modified NP were examined following incubation in mammalian growth media containing fetal bovine serum (FBS) for 1, 4, 24 and 48 hours. The protein corona transition from its early dynamic state to the later more stable corona was evaluated using mass spectrometry. The NP diameter was 22.4 ± 2.2 nm measured by scanning transmission electron microscopy (STEM). Changes in hydrodynamic diameter and agglomeration kinetics were studied using dynamic light scattering (DLS). The initial surface chemistry of the NP played an important role in the development and final composition of the protein corona, impacting agglomeration kinetics and NP toxicity. Particle toxicity, indicated by changes in membrane integrity and mitochondrial activity, was measured by lactate dehydrogenase (LDH) release and tetrazolium reduction (MTT), respectively, in mouse alveolar macrophages (RAW264.7) and mouse lung epithelial cells (C10). SiO_2-COO^- NP had a slower agglomeration rate, formed smaller aggregates, and exhibited lower cytotoxicity compared to SiO_2 and SiO_2-NH_2. Composition of the protein corona for each of the three NPs was unique, indicating a strong dependence of corona development on NP surface chemistry. This work underscores the need to understand all aspects of NP toxicity, particularly the influence of agglomeration on effective dose and particle size. Furthermore, the interplay between materials and local biological environment is emphasized and highlights the need to conduct toxicity profiling under physiologically relevant conditions that provide an appropriate estimation of material modifications that occur during exposure in natural environments

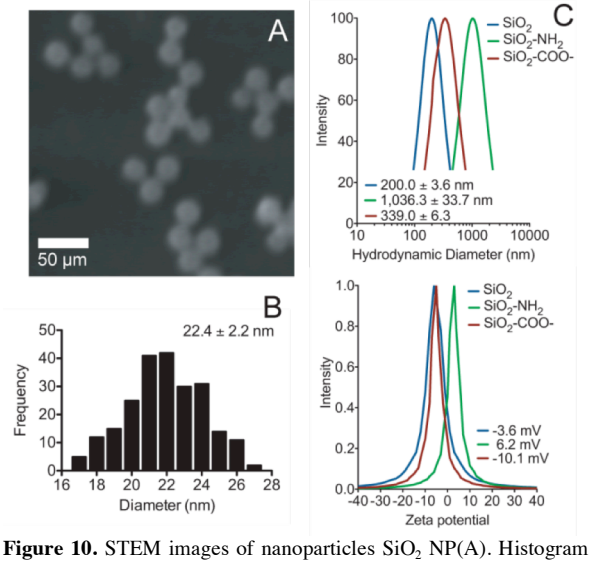

Figure 10. STEM images of nanoparticles SiO_2 NP(A). Histogram shows the distribution of nanoparticle diameter (B). Hydrodynamic diameter (C) and zeta-potential for the three NP measured in RPMI1640 (D).

Understanding the dynamic behaviour and composition of the protein corona *in vitro* and its role in nanotoxicity is essential to predicting the fate of NPs in *in vivo* systems. Here, the protein corona composition on spherical SiO_2 NPs (native surface, $-NH_2$ and $-COO^-$), physical characterization shown in Figure 10, was evaluated after 1, 4, 24 and 48 hours of incubation in mammalian cell growth media containing fetal bovine serum (FBS). Changes in diameter, zeta-potential and agglomeration state were measured. The proteins comprising the corona were identified using mass spectrometry. Subsequently, NP toxicity in macrophages (RAW264.7) and lung epithelial cells (C10) was evaluated. In both *in vitro* and *in vivo* experiments, NPs interact with the biological surfaces at different time points and are continuously exposed to the

protein-rich natural environment. The material modifications that ensue, drastically influence the physical and chemical state of the NPs, and must be understood for proper interpretation of conventional dose-response assays.

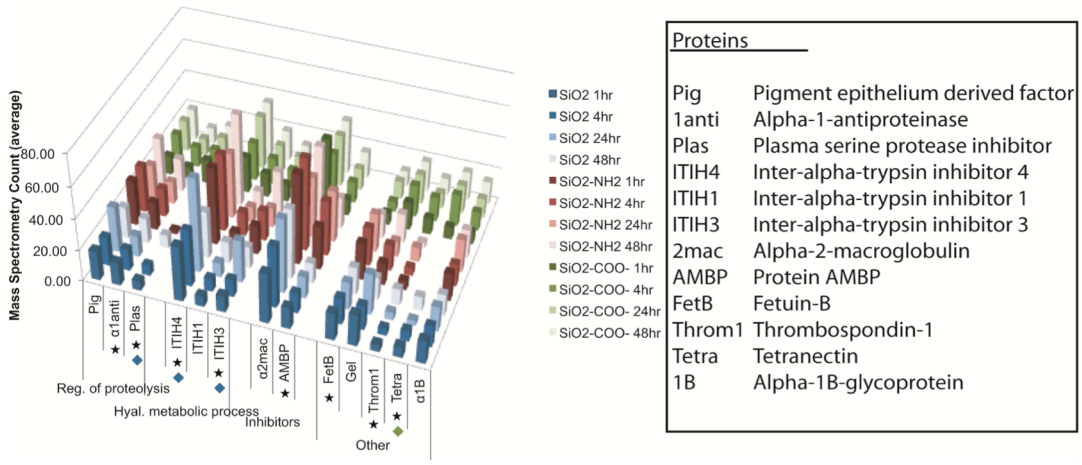

Figure 11. Mass spectrometry data showing spectrum count of proteins involved in the regulation of proteolysis, hyaluronan metabolic processes and other functions. Stars indicate statistically significant variation across NP type. Blue, Green and Red diamonds indicate statistically significant changes in for SiO2, SiO2-NH, and SiO2-COO- particles respectively over time. Additional data is shown in the full manuscript within the appendix.

The composition of the protein corona formed on NP in growth media was analyzed using mass spectrometry (MS). Identification of proteins was performed at four time points (1, 4, 24 and 48 hours) to evaluate the corona formation in complete growth media. After incubation in growth media, prior to digestion and analysis of the protein corona, NP were washed three times in PBS to remove loosely attached proteins. The MS intensities (normalized Spectrum Count exceeding a threshold) for SWISS-PROT database identified proteins are presented in the published manuscript. The proteins were grouped according to their biological function(s) listed in the SWISS-PROT database: Immune responses, transport and others (Example Figure 11).

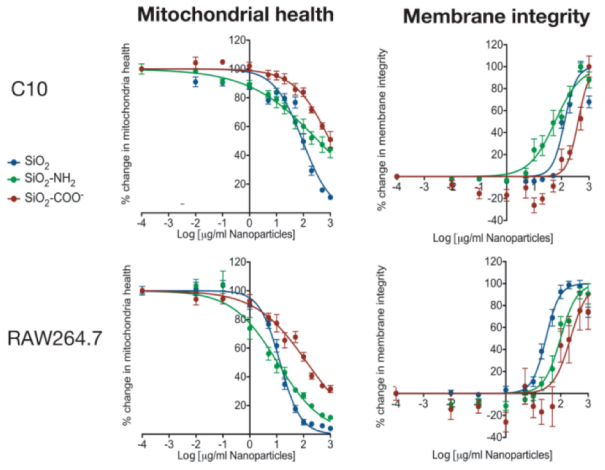

Figure 12. NP toxicity as measured by membrane integrity (LDH assay) and mitochondria health (MTT assay) for RAW264.7 and C10 cells.

Cytotoxicity induced by NP following a 24 hour exposure was examined in two mammalian cell lines, mouse alveolar macrophages (RAW264.7) and mouse lung epithelial cells (C10), Figure 12. Two commercially available assays were used to measure toxicity. LDH assays were performed to assess cell membrane integrity. A MTT assay was used to assess

mitochondrial activity. The toxicity assays were done in mammalian growth media containing FBS, and the dose-response curves for the toxicity assays ranged from 0.01 to 1000 μg/mL and were fitted to a sigmoidal dose-response (variable slope).

The dose-response study presented here showed that SiO_2-NH_2 NP were slightly more toxic than the native NP when considering mitochondrial activity, but with respect to membrane integrity native SiO_2 were the most toxic NPs. An interesting study reported in the literature tested the response in RAW264.7 cells to three polystyrene (PS) NP: native PS, PS-NH_2 and PS-COO^- [7]. Exposing RAW264.7 cells to NP in mammalian growth media containing FBS, the group revealed that PS-NH_2 NP led to the highest production of mitochondrial O_2^-, cellular H_2O_2, and hydroxyl ($OH^{\square}$), as well as increased levels of cellular and mitochondrial calcium (Ca^{2+}). This is consistent with our finding, that original NP surface chemistry influences *in vitro* NP toxicity by influencing particle agglomeration and material modification via protein adsorption. Such findings confirm that multiple mechanisms are involved in cellular responses to, and uptake of NP. These interactions are influenced by NP size, surface chemistry, material modification and cell type.

	RAW264.7		C10	
	Membrane Integrity	Mitocondrial Activity	Membrane Integrity	Mitocondrial Activity
Nanoparticles	EC_{50} (μg/ml), (Hill Coefficient)	EC_{50} (μg/ml), (Hill Coefficient)	EC_{50} (μg/ml), (Hill Coefficient)	EC_{50} (μg/ml), (Hill Coefficient)
SiO_2	28.7 (1.7)	13.4 (-1.1)	128.9 (2.0)	93.9 (-0.8)
SiO_2-NH_2	97.9 (1.5)	10.8 (-0.5)	58.2 (0.9)	361.4 (-0.3)
SiO_2-COO^-	225.2 (1.4)	134.1 (-0.5)	399.6 (2.1)	988.0 (-0.6)

Table 2. EC_{50} values and Hill coefficient for membrane integrity (LDH assay) and mitochondria health (MTT assay).

Development of *in vitro* models for understanding Cardiotoxicity

Conventional *in vitro* assays used within the pharmaceutical industry to predict cardiac toxicity rely on monolayer cultures of cardiomyocytes to screen drug candidates for adverse affects on cardiac tissue. These tissue models are inadequate and generally fail to allow accurate quantification of parameters such as force of contraction, rate of relaxation, and rate of action potential propagation, all highly sensitive measures of cardiac tissue response. Cardiac microwires, consisting of a multicellular culture of cardiomyocytes, fibroblasts and other supporting cells suspended within a collagen matrix between flexible posts provide a more physiologically relevant model of cardiac tissue response. By measuring the deflection of posts to which the cardiac tissue is suspended, contractive forces and rate of relaxation are readily quantified. These wires provide a path for developing tailored disease models for predictive toxicology.

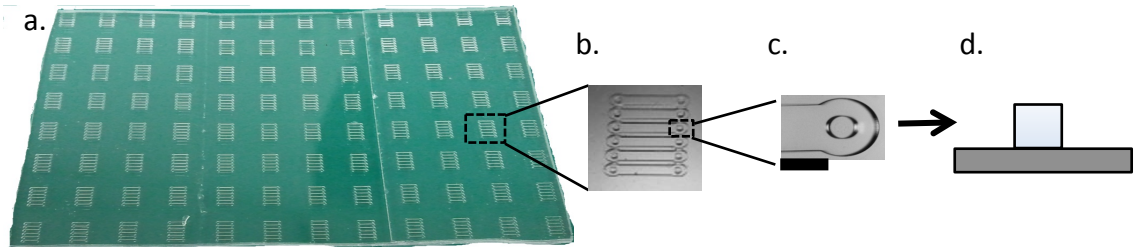

Figure 13: PDMS micropillar pair arrays in a dog bone shaped micro-well. This is a 12x8 array with each cell having 6 micro-wells. The pillars are 300 μm in diameter. Scale bar is 600 μm

There is currently a knowledge gap in understanding the impact of total contraction length on cardiac function and wire stability. 40%-50% fractional shortening is a normal predicator of healthy cardiomyocytes in an *in vivo* heart. We fabricated silicone posts created by soft lithography that can be fused with a 96 well mciro-well plate (Figure13).

It is necessary to have a 'notched' profile to allow control of the micro-wire suspension height and prevent loss of wires during contraction. It is possible in theory to fabricate SU8 mastesr that will make molds for notched PDMS pillars by controlling the exposure time used to develop the SU8 resist (Figure 14).

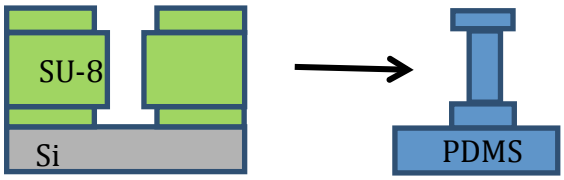

Figure 14: Schematic of a three layer SU8 master to be used as a mold to cast PDMS micro-pillars with stoppers on top. Controlled exposure will be used on layer 2 to create the mold for the pillar.

A proof of concept experiment was conducted to create SU8 bridges (Figure 3). SU8 resist was coated to a thickness of 310 mm. Pillars of diameter 300 μm were created using standard exposure time of 45 seconds. Bridges across the micro-wells were fabricated by using a 10 s exposure time. The values of exposure time used to create the bridges and the thickness of the bridges can be plugged into Equation 1 to get the critical dosage at a given exposure time and for a given depth of SU8. (Appl. Phys. Lett. **88**, 024107 (2006);

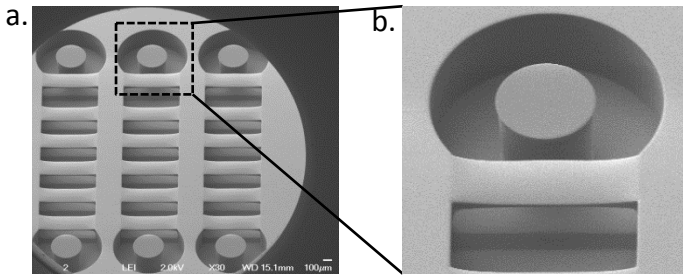

Figure 15: A proof of concept experiment to demonstrate that controlling exposure time can be used to control the depth of polymerization in SU8. Controlled exposure was used to create bridge like structures in SU8. SU8 micro-pillar pair arrays in a dog bone shaped micro-well with SU8 bridges crossing the micro-wells. Each well has a pair of pillars and 6 bridges. The pillars

http://dx.doi.org/10.1063/1.2164390)Once the critical dosage is determined, this can be used to determine the exposure time required to create exposed layers of SU8 of differing depths.

$$D(d,t_{\exp}) = \frac{(1-R_1)I_0 t_{\exp}(1+R_2 e^{-2\alpha_{Un\exp}(d_{total}-d)})(e^{-\alpha_{Un\exp}d} - e^{-\alpha_{Exp}d})}{(\alpha_{Exp} - \alpha_{Un\exp})d}$$

Equation 1: $D(d,t_{exp})$ is the critical dose at a given depth 'd' in the resist for a given exposure time t_{exp} . I_0 (mj/cm^2) is the incident light energy. R_1 is the reflectivity coefficient at the air/SU8 interface and R_2 is the reflectivity coefficient at the SU8/Silicon wafer interface. There are two absorption coefficients. α_{Exp} is the absorption coefficient for the exposed part of SU8 and α_{Unexp} is the absorption coefficient for the unexposed part of SU8. The total thicknes of the resist is indicated by d_{total}.

6x7 PDMS micro-pillar arrays were then cast with pillar diameters of 300 mm. These pillars had a base and stopper diameter of 600 μm (Figure 16).

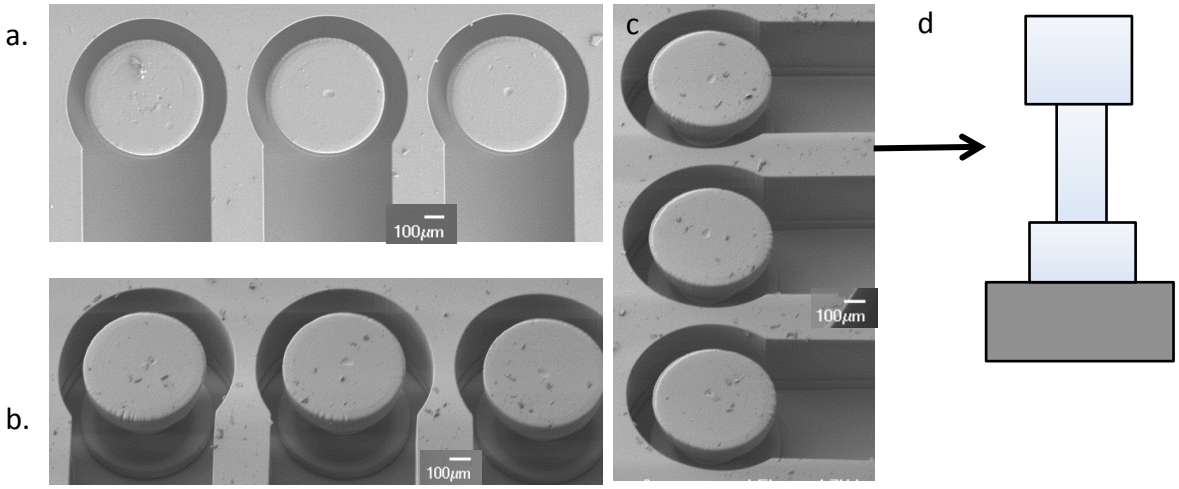

Figure 16: SEM of a PDMS micro-pillar array with stoppers on top of the pillars. The pillars are 300 mm in diameter and the stopper and base are 600 mm in diameter. (a) The micro-pillars as seen from the top. (b) The micro-pillars as imaged at a 37.5^0 tilt. (c) The micro-pillars as imaged at a 37.5^0 tilt after being rotated 90^0. Scale bars are 100 mm. The operating voltage was 1.5keV

6x7 PDMS micro-pillar arrays were also cast with pillar diameter of 150 mm. These pillars had a base and stopper of diameter 200 μm(Figure 17).

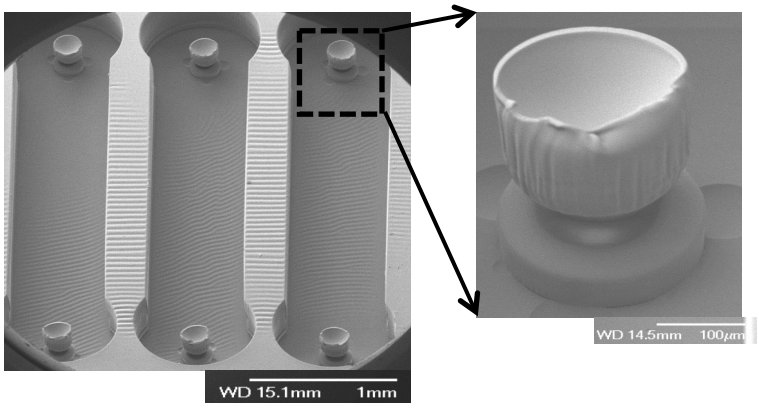

Figure 17: SEM of a PDMS micro-pillar array with stoppers on top of the pillars. The pillars are 150 mm in diameter and the stopper and base are 200 mm in diameter. The micro-pillars were imaged at a 37.5^0 tilt. The operating voltage was 1.5keV

The 300 μm diameter 6x7 PDMS micro-pillar arrays and the 200 μm diameter 6x7 PDMS micro-pillar arrays were fused to a bottomless 96 well plate (Figure 18).

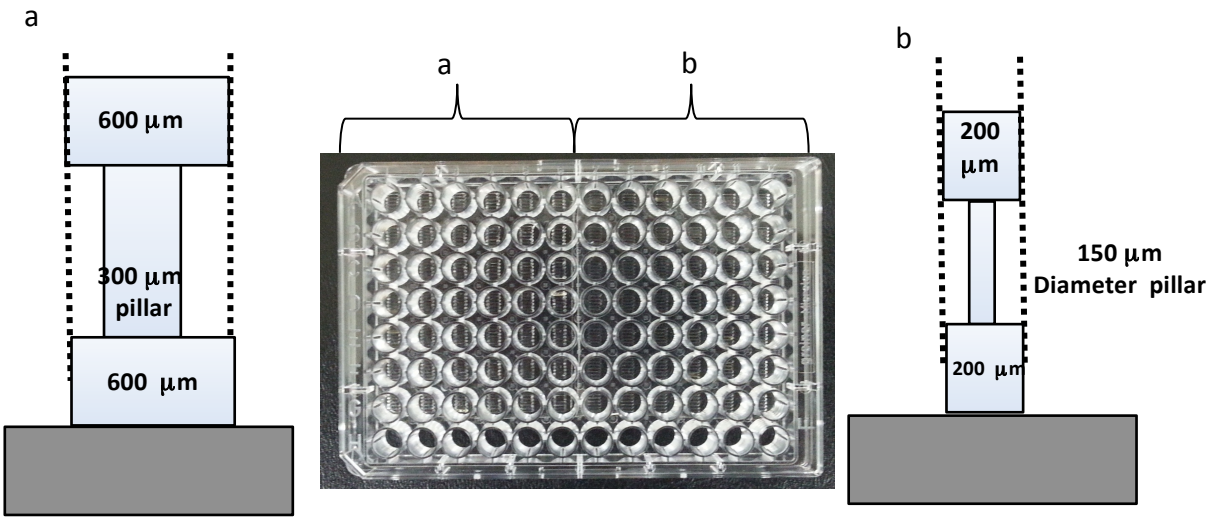

Figure 18: PDMS micro-pillar array with stoppers on top of the pillars fused to a bottomless 96 array micro-well plate. (a) 6x7 array of pillars with pillars of diameter 300 μm and the stopper and base are 600 μm in diameter. (b) 6x7 array of pillars with pillars of diameter 150 μm and the stopper and base are 200 μm in diameter.

The platform will be adaptable to integration within a microfluidic channel to facilitate active control of the chemical environment surrounding the micro-wires and will be broadly applicable to the interrogation of cardiac micro-wires.

Key questions that will be addressed using the current platform will be;
i) What is the correlation between fractional shortening, contraction force, and relaxation rate in cardiac wires?
ii) How does fractional shortening impact the sensitivity of cardiac wires to pharmaceutical intervention and changes in their local chemical environment?

Plans for Collaborations involving the BMI, ORNL, and other organizations

Moving forward, we expect to continue working with BMI, CCRM and PNNL in the development of in vitro platforms for predictive toxicology. This includes the continuation of the cardiac microwire research that is the subject of a current CNMS user proposal, "A flexible platform for monitoring the impact of fractional shortening on cardiac microwire contraction force and relaxation rate CNMS2013-151," as well as a broader class of microphysiological systems that were outlined in proposals already submitted by the team (below).

DARPA BAA 11-73, A Multi-Scale Approach to Develop an Integrated Platform of Human Microphysiological Systems
Requested Funding: $30.7M ($9.2M Base Award, 18mo.), ORNL Subcontract: $6.25M (1.25M/yr, 5 years)
Primary Contractor: Battelle Memorial Institute, M. Holsapple (PI), A. Brys (PM)
Subcontractors: Centre for Commercialization of Regenerative Medicine, PNNL, ORNL

NIH UH2/UH3 RM-11-022, Microfluidic iPS derived Cardiac Nanowire and Capillary Bed Tissue Constructs
Requested Funding: $2.2M, UH2 (2 years), $8.4M UH3 (3 years)
Primary Contractor: Battelle Memorial Institute, M. Holsapple (co-PI), P. Zandstra (co-PI)
Subcontractors: Centre for Commercialization of Regenerative Medicine, PNNL, ORNL

NIH UH2/UH3 RM-11-022, Nanostructed iPS Derived BBB and Neuronal Tissue Constructs
Requested Funding: 2.2M, UH2 (2 years), $8.4M UH3 (3 years)
Primary Contractor: Battelle Memorial Institute, M. Holsapple (PI), P. Zandstra (co-PI)
Subcontractors: Centre for Commercialization of Regenerative Medicine, PNNL, ORNL

Conclusions

The development of strategies and technologies that improve the reliability of predictions for the toxicity of materials and chemicals remains crucial to protecting human and environmental health and represents a significant opportunity for improving the therapeutic development pipeline. Within this CRADA, ORNL has led the development of new classes of well-characterized nanomaterials that have facilitated the correlation of data across molecular, cellular and whole animal scales by allowing multiple imaging modalities to be used for tracking NP transport, fate and impact in model *in vitro* systems. An internal process of physical, chemical and functional characterization, including conventional well-plate and multichannel fluorescent imaging assays, was put in place to screen and monitor NP properties throughout the duration of the project.

Subject Inventions

VOLUME-LABELED NANOPARTICLES AND METHODS OF PREPARATION
application Serial No. 12/981,886 filed December 30, 2010. This invention was made with government support under Prime Contract No. DE-AC05-00OR22725 awarded by the U.S. Department of Energy.

Commercialization Possibilities

The broad class of particles enabled by the core shell volume labeling process described above opens the door to creating new classes of optical and magnetic imaging probes that could be used in medical and basic research, drug delivery and sensor development. We continue to work with Battelle, CCRM and other MSTI members on the development of microfluidic and nanostructured platforms for high-throughput screening and predictive tox testing.

Manuscripts lead by ORNL, Generated by the Work Supported by the CRADA

W. Wang, C. Foster, J. Morrell-Falvey, P. Nallathamby, N. Mortensen, M. Doktycz, B. Gu, S. Retterer "Volume Labeling with Alexa-Fluor Dyes and Surface Functionalization of Highly Sensitive Fluorescent SiO2 Nanoparticles," Nanoscale, (Minor Revisions, resubmitted) IF 5.91

N. Mortensen, G. Hurst, W. Wang, C. Foster, P. Nallathamby, S. Retterer "Dynamic Development of the Protein Corona on Silica Nanoparticles: Composition and Role in Toxicity," Nanoscale 2013 Jul 21;5(14):6372-80. doi: 10.1039/c3nr33280b. Epub 2013 Jun 4 IF 5.91

P.D. Nallathamby, H.A. Palko, N.P. Mortensen, M. Malfatti[3], C. Smith, S.T. Retterer, and W. Wang, Unique Surface Radiolabeling Scheme of Super Paramagnetic Iron Oxide Nanoparticles (SPIONs) for Accurate Extrapolation of Pharmaco-Kinetic Distribution Studies in Life Sciences, Nanoscale (to be submitted)

Presentations Based on the Work Supported by the CRADA

S.T. Retterer, Synthesis and Analysis of Nanoparticles for Understanding Toxicity, NSRC Nanoparticle Workshop, November 2012

N. Mortensen, G. Hurst, W. Wang, C. Foster, P. Nallamthamby, S. Retterer, Protein Corona Composition and Role in the Toxicity of Silica Particles, BMES Fall Meeting, October 2012

N. Mortensen, G. Hurst, W. Wang, C. Foster, P. Nallathamby, S. Retterer, Effects of Surface Chemistry on Protein Corona Formation on Silica Nanoparticles. Society of Toxicology Annual Meeting 2012.

W.Wang, S. T. Retterer, M.J. Doktycz, B. Gu, Fabrication of Stable Multifunctional Composite Nanoparticles: Volume Labeling SiO_2 by Radioactive Isotope and Fluorescence Dyes, ACS Spring Meeting, 2012

P.D. Nallathamby, H.A. Palko, M. Malfatti, S.T. Retterer W. Wang, Bi-Mode Detectable Nanoparticles for Bio-Distribution Studies in Life Sciences, Pittcon 2013

P.D. Nallathamby, H.A. Palko, W. Wang, M. Malfatti, S.T. Retterer, Dual Mode Nanoparticles for Bio-Distribution Studies in Life Sciences, Materials Research Society 2012 Fall Meeting